Available online at www.sciencedirect.com
ScienceDirect
Applied Catalysis A: General 319 (2007) 98–110
APPLIED CATALYSIS A: GENERAL
www.elsevier.com/locate/apcata

Influence of reaction conditions on catalyst composition and selective/non-selective reaction pathways of the ODP reaction over V_2O_3, VO_2 and V_2O_5 with O_2 and N_2O

Evgenii V. Kondratenko *, Olga Ovsitser, Joerg Radnik, Matthias Schneider, Ralph Kraehnert, Uwe Dingerdissen

Leibniz-Institut für Katalyse e. V. an der Universität Rostock, Aussenstelle Berlin, Richard-Willstätter-Str. 12, D-12489 Berlin, Germany[1]

Received 8 September 2006; received in revised form 16 November 2006; accepted 17 November 2006
Available online 18 December 2006

Abstract

The effect of reaction conditions on catalytic performance and composition of individual vanadium oxides (V_2O_3, VO_2, and V_2O_5) in the oxidative dehydrogenation of propane (ODP) at 773 K was investigated by means of steady-state catalytic experiments with $^{16}O_2$, $^{18}O_2$ and N_2O in combination with in situ XRD, in situ UV–vis, and ex situ XPS analysis. Steady-state product selectivities over these oxides are not determined by their initial (fresh) composition but a new catalyst composition created under the reaction conditions. At similar degrees of propane conversion, this steady-state composition depends on the oxidizing agent (O_2 or N_2O). For an oxygen ($C_3H_8/O_2 = 2$) containing mixture ($X(C_3H_8) < 5\%$, $X(O_2) < 10\%$), vanadium species are stabilized in penta- and tetravalent oxidation states, with the former being the main one. In the presence of N_2O, the oxidation state of vanadium is lower under controlled degrees of propane and oxidant conversion ($X(C_3H_8) < 5\%$, $X(N_2O) < 10\%$). It is suggested that the difference in the oxidation state of vanadium with O_2 and N_2O is related to the lower ability of N_2O for reoxidation of reduced VO_x species as compared to O_2. Moreover, individual vanadium oxides poorly performing with O_2 become selective in the ODP reaction using N_2O. This improving effect of N_2O on the catalytic performance of vanadium oxides is related to the degree of catalyst reduction under reaction conditions and to the nature of oxygen species originated from O_2 and N_2O.

Keywords: Propane; Propene; N_2O; Reaction mechanism; ODP; XRD; XPS; UV–vis; SSITKA

1. Introduction

Oxidative selective catalytic utilisation of low alkanes (ethane and propane) continues to be an actual topic of research studies due to increased demands for olefins and oxygenates. The relevant results have been recently reviewed [1–4]. For the oxidative dehydrogenation of propane to propene (ODP), vanadium- and molybdenum-based oxide catalysts belong to the best-performing catalytic materials using O_2 as oxidizing agent. Unfortunately, the present-day catalytic materials suffer from low propene selectivities at high degrees of propane conversion due to higher reactivity of propene as compared to propane. In our recent studies of the ODP reaction over VO_x/γ-Al_2O_3 [5] and VO_x/MCM-41 [6] catalytic materials it was demonstrated that propene selectivity could be increased when O_2 was replaced by N_2O. The most significant improvements in propene selectivity (up to three times) were achieved for the sample possessing bulk like V_2O_5 species. It was suggested that the improved ODP performance with N_2O was due to the lower ability of N_2O for re-oxidation of reduced VO_x species, i.e. the degree of catalyst reduction in the presence of N_2O is higher than in the presence of O_2.

The importance of different oxidation states of vanadium has been mentioned for various catalytic oxidation reactions [7–13]. In a recent study of Schlögl and co-workers [14], it was shown that morphological and electronic changes of V_xO_y nanoparticles under conditions of partial oxidation of *n*-butane played an important role in the catalytic reaction.

Moreover, for catalytic tests in continuous flow fixed-bed reactors, concentration gradients of feed components and reaction products are observed in the catalyst bed. This results

* Corresponding author. Tel.: +49 30 63924448; fax: +49 30 63924454.
E-mail address: evgenii@aca-berlin.de (E.V. Kondratenko).
[1] Former Institute for Applied Chemistry Berlin-Adlershof.

0926-860X/$ – see front matter © 2006 Elsevier B.V. All rights reserved.
doi:10.1016/j.apcata.2006.11.021

in a variation of the catalyst composition in different parts of the reactor. Barbero et al. [11] identified three different catalyst compositions along the catalyst bed after performing the ODP reaction with O_2 over V_2O_5 at 823 K. At the reactor inlet, where O_2 and C_3H_8 were present at the ratio of 1, V_2O_5 was stabilized. Upon passing the reaction feed and products down-stream over the catalyst, the catalyst composition changed from V_2O_5 to VO_2 and finally to V_2O_3. The changes were explained by the fact that the ratio of C_3H_8/O_2 increased along the catalyst bed due to enhanced consumption of O_2 as compared to C_3H_8. Since the reaction atmosphere becomes more reduced down-stream of the catalyst, V_2O_5 is reduced to lower valence vanadium oxides. However, these authors [11] did not report any catalytic data.

In order to adequately establish structure–reactivity/selectivity relationships in the ODP reaction, catalyst characterization and catalytic tests should be performed under controlled reaction conditions, i.e. minimized concentration gradients of feed components in the catalyst bed. To the best of the author's knowledge, there are no comprehensive studies of a structure-selectivity relationship for individual vanadium oxides (V_2O_5, VO_2 and V_2O_3) in the ODP reaction with O_2 and N_2O. These systems are considered to be models for elucidating the role of differently oxidized vanadium species in selective and non-selective ODP reaction pathways.

The present study is focused on the effect of different oxidizing agents (O_2 and N_2O) on ODP catalytic performance of individual vanadium oxides. Particular attention is paid to the role of reaction-induced surface and bulk changes of V_2O_3, VO_2 and V_2O_5. To this end, steady-state ODP performance of V_2O_3, VO_2 and V_2O_5 with O_2 and N_2O was determined and compared with the results of characterization studies by means of in situ UV–vis, in situ XRD and ex situ XPS. Mechanistic insights into the role of O_2 in CO_2 formation in the ODP reaction were derived from SSITKA (steady-state-isotopic-transient-kinetic-analysis) tests. The obtained knowledge may be eventual helpful to design improved catalysts.

2. Experimental

2.1. Catalysts and their characterization

Nitrogen physisorption was employed to obtain specific surface areas in a single point BET analyzer (Gemini III 2375, Micromeritics) by using N_2 physisorption at 77 K. The BET values of fresh V_2O_5 (99.6%, Aldrich), VO_2 (99.5%, ChemPur) and V_2O_3 (99.9%, ChemPur) are 9.7, 11.6 and 7.3 m^2/g, respectively.

The crystalline bulk composition of vanadium oxides during the ODP reaction was determined by means of in situ XRD using a theta theta powder diffractometer (Seifert) with multilayer mirror and Cu $K\alpha_1$ radiation. Undiluted catalyst samples (ca. 50 mg) were placed on the Pt–Rh sample holder of the in situ XRD cell (Bühler HDKS1). The holder was coated with Au prior to experiments, in order to suppress blank activity of Pt–Rh for the ODP reaction at 773 K. The degree of propane conversion over the coated holder at 773 K did not exceed 0.1%. The catalytic samples were studied using either $C_3H_8/O_2/Ne = 40/20/40$ or $C_3H_8/N_2O/Ne = 40/40/20$ reaction feeds at 1 bar and 773 K for 4 h (total flow of 60 ml(STP)/min). A fresh sample was used for each experiment. The in situ XRD patterns were recorded every ca. 15 min.

In order to determine near-to-surface composition of used catalytic materials by XPS, an ESCALAB 220i-XL spectrometer (Fisons Instruments) with Mg Kα radiation (1253.3 eV) was applied. The ex situ XPS study was performed in the following way. The samples (20–50 mg) diluted with quartz particles were treated in oxygen ($C_3H_8/O_2/Ne = 40/20/40$) or N_2O ($C_3H_8/N_2O/Ne = 40/40/20$) containing reaction feeds at 1 bar and 773 K for 4 h. The degrees of propane and oxidant conversion did not exceed 5 and 10%, respectively. After the catalytic reaction, the samples were cooled down to 300 K in the same gas flow, and transferred in air to the sample holder for XPS measurements.

In situ UV–vis experiments were performed to follow the changes in reduction state of individual vanadium oxides under reaction conditions with different oxidants (O_2 and N_2O). In situ UV–vis spectra were recorded under reaction conditions while passing different reaction mixtures ($C_3H_8/O_2/N_2 = 40/20/40$ and $C_3H_8/N_2O/Ne = 40/40/20$) through the catalyst bed at 773 K. The total gas flow was kept at 40 ml(STP)/min. In order to have a sufficient catalyst bed length (2–3 mm) for spectroscopic studies and to keep the propane conversion under 5%, the catalyst was slightly diluted with quartz particles. A thermocouple inside the catalyst bed was used to control the reaction temperature. The in situ UV–vis analysis was performed using an AVASPEC fiber optical spectrometer (Avantes) equipped with a DH-2000 deuterium-halogen light source and a CCD array detector. A high-temperature reflection probe consisting of six radiating and one reading optical fibers was located inside the furnace perpendicular to the reactor. The sensor was connected to the spectrometer and the light source by fiber optical cables (length 2 m) consisting of a core of pure silica (diameter 0.4 mm) coated with polyimide. The spectra were converted into the Kubelka–Munk function $F(R)$.

2.2. Catalytic tests

A U-shaped fixed-bed quartz reactor (i.d. 5 mm) was employed for the catalytic tests. The quartz reactor was immersed into a fluidized bed of sand serving as a source of heat or its removal. The temperature within the fixed-bed of catalyst particles was measured by an axially movable thermocouple located inside a quartz capillary. Catalyst was diluted with quartz particles to assure temperature control. The oxidative conversion of propane was investigated using $C_3H_8/N_2O/Ne = 40/40/20$, $C_3H_8/O_2/Ne = 40/20/40$, and $C_3H_8/O_2/Ne = 40/10/50$ feeds at 1 bar and 773 K. Neon was used to control the formation of N_2 and O_2 in case of N_2O decomposition. In order to achieve different degrees of propane conversion, the total flow rates and catalyst amounts were varied between 30 and 240 ml(STP) min^{-1} and between 5 and

200 mg, respectively. The feed components and products were analyzed using an online GC (HP 5890) equipped with Porapak Q and Molecular sieve-5 columns.

The steady-state isotopic transient kinetic analysis (SSITKA) experiments were performed in a tubular quartz reactor at 1 bar and 773 K. Catalyst amount and gas flows were fixed to 85 mg and 40 ml(STP) min^{-1}, respectively. The following reaction feeds were used: $^{16}O_2$/Ne/Ar = 2/2/96, $^{18}O_2$/Ne/Ar = 2/2/96, $C_3H_8/^{16}O_2$/Ne/Ar = 4/2/2/92, and $C_3H_8/^{18}O_2$/Ne/Ar = 4/2/2/92. Oxygen tracing experiments were performed by switching from non-labeled to labeled reaction feeds after a pseudo steady-state operation. The gas composition at the reactor outlet was monitored by on-line mass spectrometry (Balzer Omnistar). The following atomic mass units (AMUs) were analyzed: 48 ($C^{18}O_2$), 46 ($C^{18}O^{16}O$), 44 ($C^{16}O_2$, C_3H_8), 42 (C_3H_6, C_3H_8), 40 (Ar), 36 ($^{18}O_2$), 34 ($^{16}O^{18}O$), 32 (O_2), 30 ($C^{18}O$, C_3H_8), 29 (C_3H_8), 28 ($C^{16}O$, $C^{16}O_2$, C_3H_8, C_3H_6), 20 (Ne, $H_2{}^{18}O$), and 18 ($H_2{}^{16}O$). The concentration of feed components and products was determined from the respective AMUs using fragmentation patterns and sensitivity factors, which arise from the different ionization probabilities of individual compounds. The relative sensitivities were determined as a ratio of the intensity of the mass spectrometry signal of each compound related to that of Ar (inert standard). The respective intensities were corrected according to the contribution of fragmentation pattern of other compounds to the measured AMU signal. The fragmentation patterns and respective sensitivities of feed components and reaction products were determined from separate calibration experiments, where a mixture of reference gas and inert standard was introduced into the reactor filled with SiO_2 particles. It was assumed that there is no difference in the calibration values between the non-isotopically and isotopically labeled compounds.

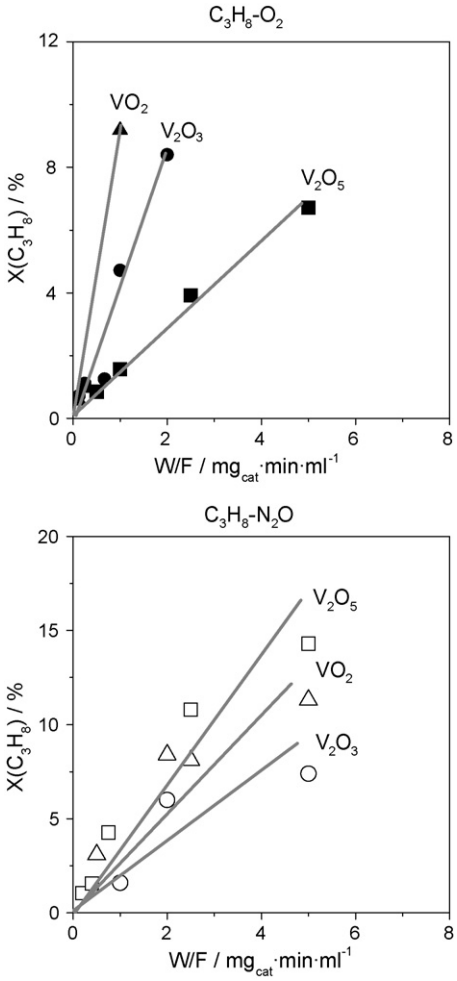

Fig. 1. Propane conversion vs. contact time (W/F) over V_2O_5 (■, □), VO_2 (▲, △) and V_2O_3 (●, ○) (T = 773 K, $C_3H_8/O_2/Ne$ = 40/20/40 or $C_3H_8/N_2O/Ne$ = 40/40/20). Different oxidizing agents are represented by solid symbols (O_2) and open symbols (N_2O).

3. Results and discussion

3.1. Catalytic performance of V_2O_5, VO_2 and V_2O_3 with O_2 and N_2O

Catalytic performance of V_2O_3, VO_2 and V_2O_5 in the oxidative dehydrogenation of propane (ODP) was determined at 773 K for various contact times using O_2 and N_2O as oxidants. For both oxidizing agents, C_3H_6, CO and CO_2 were the main carbon-containing reaction products. Small amounts of ethylene, methane and oxygenates (acroleine, acetaldehyde) were observed at high degrees of propane conversion. Insights into the catalytic activity of different vanadium oxides in the ODP reaction can be derived from conversion-contact time plots in Fig. 1. It should be particularly stressed that the experimental data in this figure were obtained after at least 2 h on stream. This time was sufficient to achieve a pseudo steady-state operation. From the results in Fig. 1 for an O_2-containing reaction feed, it is expected that the activity of V_2O_5 for propane conversion is lower than that of V_2O_3 and VO_2. When O_2 is replaced by N_2O, V_2O_3 shows the lowest activity, while that of V_2O_5 and VO_2 are similar. At this stage it is important to note that the individual vanadium oxides were strongly restructured under reaction conditions (see Sections 3.2 and 3.3). This means that their specific surface areas may be changed. It is well accepted that for correct comparison of activity of different materials in heterogen-catalyzed reactions, the catalytic activity should be related either to the number of active sites or to specific surface. However, we were not able to determine one of these parameters after the catalytic reaction due to very low catalyst amounts used. Therefore, the data on catalytic activity of different vanadium oxides in Fig. 1 should be treated with care keeping in the mind strong catalyst restructuring under reaction conditions. In contrast to the catalytic activity, it is not important to know the number of active catalyst sites or specific surface area for calculating product selectivities. Therefore, we discuss below selectivity–conversion relationships of individual vanadium oxides in the ODP reaction using O_2 and N_2O. The respective results are presented in Fig. 2.

One of the most important observations from this figure is the fact, that the selectivity–conversion plot is not influenced by the initial catalyst composition (V_2O_3, VO_2 and V_2O_5), but by the applied oxidizing agent (O_2 or N_2O). At comparable

degrees of propane conversion, propene selectivity is higher with N_2O than with O_2. This coincides with our previous analysis of the ODP reaction over differently loaded VO_x/MCM-41 [6] and VO_x/γ-Al_2O_3 [5] catalytic materials. A possible explanation for the observed phenomena is given in Section 3.3.

For both oxidizing agents, propene selectivity decreases with an increase in propane conversion. This is due to a consecutive C_3H_6 oxidation to CO and CO_2. However, these non-selective reaction pathways are influenced by the nature of oxidizing agent. From the results in Fig. 2(a) it is clear that propene selectivity decreases with an increase in the degree of propane conversion stronger with O_2 than with N_2O. For an O_2-containing reaction feed, C_3H_6 selectivity decreases from 77 to 15% upon increasing C_3H_8 conversion from 0.6 to 9%. For similar changes in the degree of C_3H_8 conversion in the presence of N_2O, C_3H_6 selectivity drops only from 86 to 60%. These findings evidence that consecutive propene oxidation to CO_x is suppressed upon replacing O_2 with N_2O.

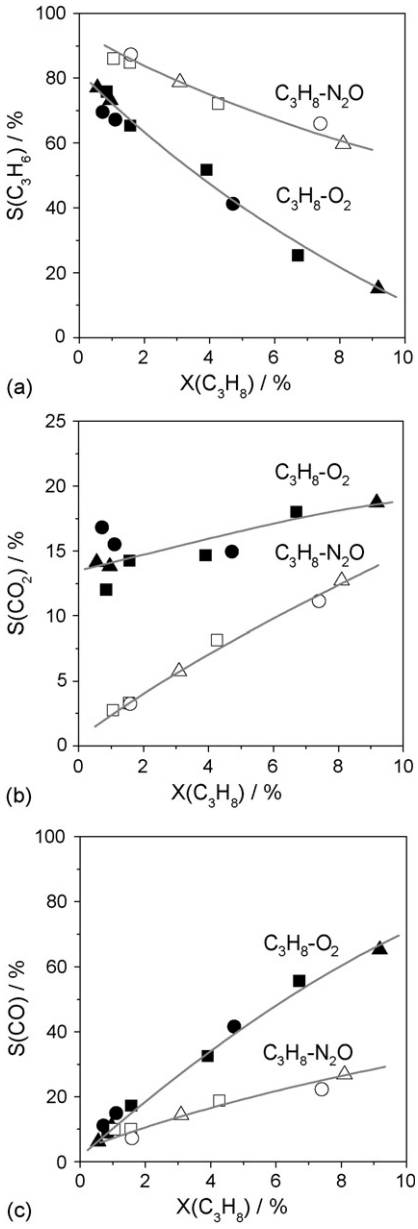

Fig. 2. Selectivity of C_3H_6 (a), CO_2 (b) and CO (c) measured at different degrees of propane conversion over V_2O_5 (■, □), VO_2 (▲, △) and V_2O_3 (●, ○) (T = 773 K, $C_3H_8/O_2/Ne$ = 40/20/40 or $C_3H_8/N_2O/Ne$ = 40/40/20). Different oxidizing agents are represented by solid symbols (O_2) and open symbols (N_2O).

The reaction pathways of CO and CO_2 formation are also influenced by the nature of oxidizing agent. It is clearly seen from the selectivity–conversion plot in Fig. 2(b) that CO_2 selectivity only slightly changes with varying degree of C_3H_8 conversion when O_2 is used as oxidizing agent. It increases from 15 to 20% upon increasing C_3H_8 conversion from 0.6 to 9%. About 13% CO_2 selectivity is expected upon extrapolation to a zero degree of propane conversion. Based on this observation and taking into account the small change of CO_2 selectivity with varying degree of propane conversion in Fig. 2(b), it is concluded that carbon dioxide is mainly formed via direct propane combustion but not via consecutive propene oxidation. The latter reaction contributes to the total CO_2 production only at high degrees of propane conversion. When O_2 is replaced by N_2O, CO_2 selectivity decreases in the studied range of propane conversions (Fig. 2(b)). The decrease in CO_2 selectivity is explained by a reduced tendency towards direct propane combustion. This conclusion is based on the fact, that a near-to-zero CO_2 selectivity is expected for a zero degree of propane conversion in the presence of N_2O (Fig. 2(b)). Upon increasing C_3H_8 conversion, CO_2 selectivity increases, hence, CO_2 is mainly formed via consecutive C_3H_6 oxidation when N_2O is used as oxidizing agent.

The selectivity–conversion plot in Fig. 2(c) evidences that CO formation is stronger influenced by the degree of C_3H_8 conversion than CO_2 formation. CO selectivity is very low (<5%) at zero C_3H_8 conversion but strongly increases with C_3H_8 conversion for both oxidants (N_2O and O_2). The obtained relationship indicates the secondary nature of CO formation, i.e. CO is formed via consecutive C_3H_6 oxidation. From Fig. 2(c) it is concluded that CO formation with O_2 is stronger influenced by the degree of C_3H_8 conversion as compared to the tests with N_2O. For an O_2-containing feed, a relative difference in CO selectivity is 60% upon increasing C_3H_8 conversion from 0.6 to 9%, while the respective difference with N_2O is 20%.

Summarizing the above discussion, it is concluded that catalytic performance and general scheme of the ODP reaction are determined by the applied oxidizing agent (O_2 and N_2O), but not by the initial composition of individual vanadium oxides. In order to identify possible reasons for the observed phenomena, a detailed catalyst characterization study was performed. The results are presented and discussed below.

3.2. Influence of reaction conditions on catalyst composition

Near surface and bulk composition of individual vanadium oxides before, during and after the ODP reaction with O_2 and N_2O were investigated by means of ex situ XPS, in situ UV–vis

and in situ XRD. The advantages of the applied in situ UV–vis and in situ XRD methods are that they were performed under real and controlled reaction conditions, i.e. $T = 773$ K, $P_{total} = 1$ bar and the degree of C_3H_8 and O_2 (N_2O) conversion below 5 and 10%, respectively. This experimental restriction is important, in order to ensure a near to uniform composition of the studied catalysts along the catalyst bed. The applied in situ UV–vis and in situ XRD techniques provide information on reaction-induced changes of bulk composition in the depth range of few micro-, and millimeters, respectively. The more surface sensitive XPS measurements were conducted ex situ, since in situ XPS requires low pressures, i.e. very different from the reaction conditions. In the following two sections, reaction-induced changes in the bulk and near surface composition of V_2O_5, VO_2, and V_2O_3 are discussed.

3.2.1. Bulk composition and structure

Fig. 3 summarises in situ XRD patterns of fresh vanadium oxides and after 4 h on stream in C_3H_8–O_2 and C_3H_8–N_2O reaction mixtures at 773 K. The detected phases and their relative ratios are presented in Table 1. From Fig. 3 it is clear that the bulk state of V_2O_5 is not significantly changed during propane oxidation with O_2. This observation disagrees with previously reported results of 1-penten oxidation over V_2O_5 [9]. However, these authors [9] did not report the degrees of 1-penten and oxygen consumption. They mentioned only that oxygen was not completely consumed. If the ratio of 1-pentane/oxygen at the reactor outlet deviated strongly from that at the reactor inlet, significant catalyst restructuring in the down stream position of the catalyst would be expected, which would explain the deviation from our results. In contrast to V_2O_5, VO_2 and V_2O_3 are restructured under the conditions of the ODP reaction with O_2 towards a more oxidized state (Fig. 3). Crystalline V_2O_5 and V_3O_7 were identified in the two latter samples, with the former being the main phase (Table 1).

When the ODP reaction was performed with N_2O, significant bulk restructuring was observed in all individual vanadium oxides. As shown in Fig. 3 and in Table 1, V_2O_3 is transformed to VO_2 and V_3O_7. The relative ratio of these phases was calculated to be 20. The same dominating phase was also identified in VO_2 after the catalytic reaction with N_2O. Fig. 3 nicely demonstrates that V_2O_5 undergoes a reductive transformation to VO_2, V_3O_7 and V_3O_5 during the ODP reaction at 773 K with N_2O. Thus, it is obvious that the bulk composition of V_2O_3, VO_2 and V_2O_5 is strongly changed under conditions of the ODP reaction (Table 1); at low degrees of propane conversion (<5%) the steady-state bulk composition of the studied vanadium oxides is determined by the nature of oxidizing agent (O_2 or N_2O).

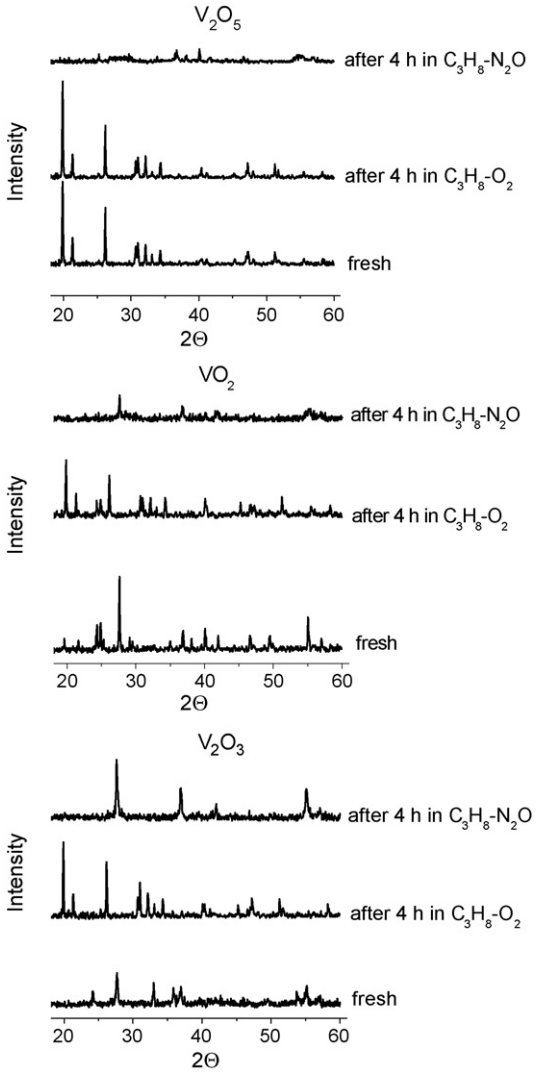

Fig. 3. In situ XRD patters of V_2O_5, VO_2 and V_2O_3: fresh as well as after 4 h in the ODP reaction with O_2 or N_2O at 773 K. $C_3H_8/O_2/Ne = 40/20/40$ or $C_3H_8/N_2O/Ne = 40/40/20$, $X(C_3H_8) < 5\%$, $X(O_2) < 10\%$, $X(N_2O) < 10\%$.

Further insights into the above-described phase transformations were derived from the temporal changes in the XRD patters during the ODP reaction with various oxidizing agents. Selected results for V_2O_3, VO_2 and V_2O_5 are presented in Fig. 4. The respective crystalline phase compositions are shown in Table 2. For V_2O_5 in a C_3H_8–N_2O flow at 773 K, the main phase changes occur already during the first 15 min on stream.

Table 1
Bulk composition (estimated values) derived from in situ XRD analysis of different vanadium oxides in fresh state as well as during ODP with O_2 and N_2O at $T = 773$ K ($X(C_3H_8) < 5\%$, $X(O_2) < 10\%$, $X(N_2O) < 10\%$)

Catalysts	Crystalline bulk phases from XRD		
	Fresh	After ODP with $C_3H_8/O_2/Ne = 40/20/40$	After ODP with $C_3H_8/N_2O/Ne = 40/40/20$
V_2O_5	V_2O_5	V_2O_5 traces of V_3O_7	VO_2, V_3O_7, V_3O_5 (low crystallinity)
VO_2	$VO_2/V_3O_7 \sim 1$	$V_2O_5/V_3O_7 = 3.3$	$VO_2/V_3O_5 = 8$
V_2O_3	V_2O_3	$V_2O_5/V_3O_7 = 9$	$VO_2/V_3O_7 = 20$

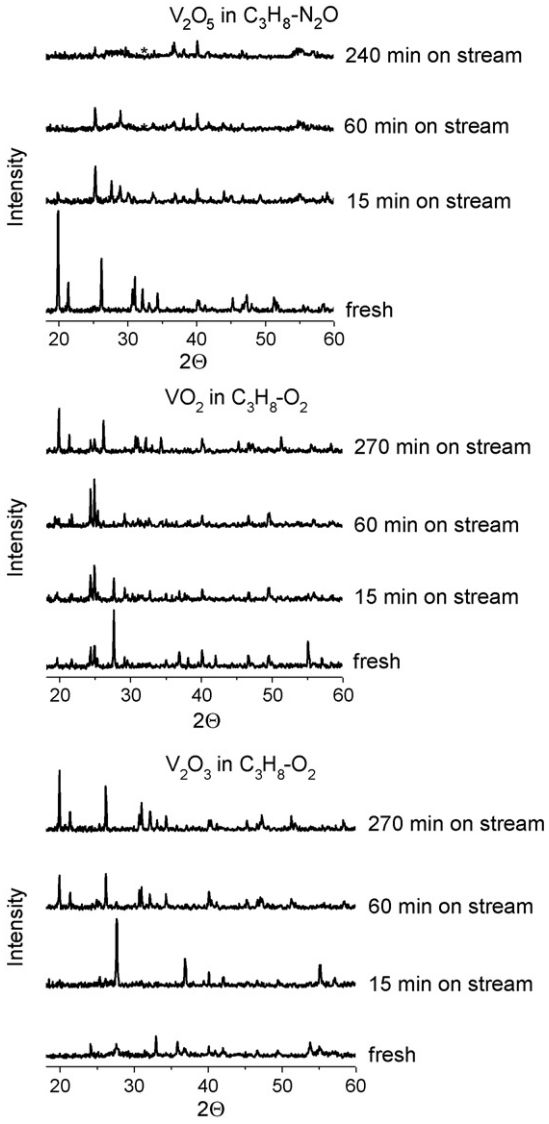

Fig. 4. Temporal changes in XRD patters of V_2O_5, VO_2 and V_2O_3 during the ODP reaction with O_2 or N_2O at 773 K. $C_3H_8/O_2/Ne$ = 40/20/40 or $C_3H_8/N_2O/Ne$ = 40/40/20, $X(C_3H_8) < 5\%$, $X(O_2) < 10\%$, $X(N_2O) < 10\%$.

V_2O_3 in a C_3H_8–O_2 flow at 773 K transforms initially to VO_2, which is further converted to V_3O_7 and V_2O_5. This proceeds during ca. 1 h on stream. In comparison to V_2O_3, VO_2 transforms slower to V_3O_7 and V_2O_5 in a C_3H_8–O_2 flow at 773 K.

In situ UV–vis analysis, which provides information on the oxidation state of vanadium species within few micro-meters in the catalyst bulk, confirms a higher reduction degree of near surface vanadium under C_3H_8–N_2O conditions as compared to C_3H_8–O_2 conditions. Fig. 5 exemplifies in situ UV–vis spectra of V_2O_5 at 773 K under different reaction conditions: (a) in an O_2 flow (O_2/Ne = 20/80), (b) in a C_3H_8–O_2 flow (C_3H_8/O_2/Ne = 40/20/40) for 60 min and (c) in a C_3H_8–N_2O flow (C_3H_8/N_2O/Ne = 40/40/20) for 10 min and (d) in C_3H_8–N_2O flow (C_3H_8/N_2O/Ne = 40/40/20) for 90 min. It is important to stress, that during these experiments the position on the UV–vis fiber, total flow, reaction temperature and pressure were not changed.

Table 2
Bulk composition (estimated values) at different times-on-stream during in situ XRD measurements at 773 K in C_3H_8–O_2 and C_3H_8–N_2O flows ($X(C_3H_8) < 5\%$, $X(O_2) < 10\%$, $X(N_2O) < 10\%$).

t (min)	Crystalline bulk phases from in situ XRD (%)				
	V_2O_3	V_3O_5	VO_2	V_3O_7	V_2O_5
ODP with N_2O over V_2O_5 (C_3H_8/N_2O/Ne = 40/40/20)					
0					100
15		11		62	26
60			30	52	18
270		44	36	20	
ODP with O_2 over VO_2 (C_3H_8/O_2/Ne = 40/20/40)					
0			52	48	
15			23	77	
60				95	5
270				20	80
ODP with O_2 over V_2O_3 (C_3H_8/O_2/Ne = 40/20/40)					
0	100				
15		5	84	3	9
60			11	20	70
270				10	90

Therefore, the discussed changes in the UV–vis spectra relate exclusively to the change of the catalyst under different reaction conditions. To keep the propane conversion under 5%, we had to use only 10 mg of V_2O_5 (fraction 0.2–0.3 mm) and mixed it with quartz of the same particle size, slightly degrading the quality of the UV–vis spectra. Fig. 5 shows the Kubelka–Munk function of V_2O_5 under O_2 and C_3H_8–O_2 flows. The Kubelka–Munk function in the range of 600–800 nm in spectra (a) and (b) is lower than in a C_3H_8–N_2O flow (spectra (c) and (d)). From spectra (c) and (d) in Fig. 5, we can conclude that there is no significant difference between spectra of V_2O_5 after 10 and 90 min on stream under C_3H_8–N_2O conditions. If coke deposits would be responsible for the absorbance between 600 and 800 nm, an increase in the absorbance is expected with time on stream. However, the UV–vis spectra after 10 and 90 min are

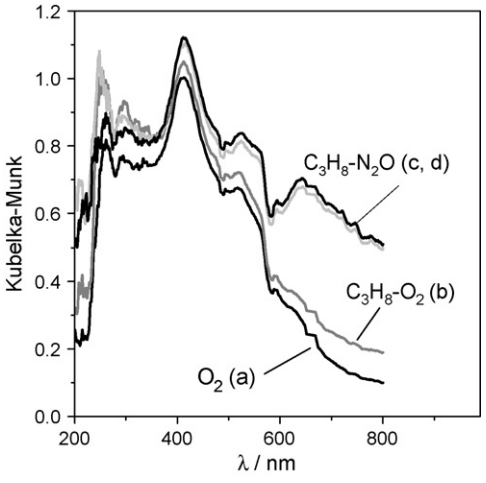

Fig. 5. UV–vis spectra of V_2O_5 at T = 773 K: (a) O_2/Ne = 20/80, black line; (b) C_3H_8/O_2/Ne = 40/20/40 after 60 min stream ($X(C_3H_8)$ = 2% and $X(O_2)$ = 5%), grey line; (c) C_3H_8/N_2O/Ne = 40/40/20, 10 min, light grey line; (d) C_3H_8/N_2O/Ne = 40/40/20 after 90 min on steam ($X(C_3H_8)$ = 1% and $X(N_2O)$ = 6%), black line.

very similar. Moreover, the ex situ XPS study does not reveal any difference in coke deposits between samples after C_3H_8–O_2 and C_3H_8–N_2O interactions at 773 K. Based on these facts we suggest that the difference between the UV–vis spectra in C_3H_8–O_2 and C_3H_8–N_2O flows indicates different reduction degrees of vanadium under the various reaction conditions, with a stronger reduced one observed for the C_3H_8–N_2O mixture. Moreover, since the UV–vis spectra of V_2O_5 after 10 and 90 min on stream in an C_3H_8–N_2O flow at 773 K are very similar to each other, but different from one in O_2 flow we can conclude that reduction of near surface layers of V_2O_5 is a rapid process. This result nicely agrees with our time-resolved XRD results in Fig. 4, and Table 2, where the reduction of V_2O_5 to V_3O_7 and V_3O_5 occurred within less than 15 min.

On this stage it is important to note that the above discussion was related to the bulk properties of vanadium oxides. However, the catalytic processes occur on the catalyst surface. Therefore, it is also essential to elucidate how the near surface composition of V_2O_3, VO_2 and V_2O_5 is influenced by the oxidizing agent (O_2 and N_2O) during the ODP reaction. To this end we applied ex-situ XPS. The obtained results are presented and discussed in the next section.

3.2.2. Oxidation state of near surface vanadium

The XP spectra of the V 2p and O 1s regions of fresh individual vanadium oxides and after performing the ODP reaction with O_2 or N_2O at 773 K are compared in Fig. 6. All spectra were referenced to the C 1s peak at 284.8 eV. During the XPS measurements no further reduction of V species was observed under the chosen conditions (I_{em} = 10 mA; U = 10 kV). Corresponding to the reaction-induced bulk changes of individual vanadium oxides (Fig. 3), also the near surface oxidation state of vanadium changed during the ODP reaction (Fig. 6, Table 3). The near surface changes are determined by the nature of the applied oxidizing agent (O_2 or N_2O). In order to quantify the influence of the oxidizing agent on the oxidation state of vanadium under the ODP conditions, the valence state of vanadium was determined taking the V $2p_{3/2}$ peak into account. To this end, the V $2p_{3/2}$ peaks were fitted with Gaussian–Lorentzian curves after Shirley background subtraction. V^{5+}, V^{4+}, and V^{3+} oxidation states were identified at V $2p_{3/2}$ electron binding energies of 517.2, 516.0, and 514.0 eV, respectively. The presently assigned binding energies for V^{5+} and V^{4+} of 517.2 and 516.0 eV are in agreement with previously published values for V_2O_5 and VO_2 [15–18]. The electron binding energy of the state correlated with V^{3+} in the present work is ca. 1 eV lower than the values known from the literature for V_2O_3 [17,19]. However, it should be stressed that the literature values were obtained for thin V_2O_3 films on metallic substrate and V_2O_3 created via reduction of V^{5+} or V^{4+} by electron bombardment. The latter samples were free of water or hydroxyls, which can influence the binding energy of V^{3+}. These adsorbates, however, do really exist in our sample used for the ODP reaction at 773 K. This might be a reason for the deviation of the presently determined binging energy for V^{3+} from that previously reported for ideal systems [17,19]. The relative concentrations of V^{5+}, V^{4+}, and V^{3+} are compared in Table 3 for fresh (non-used for the ODP reaction)

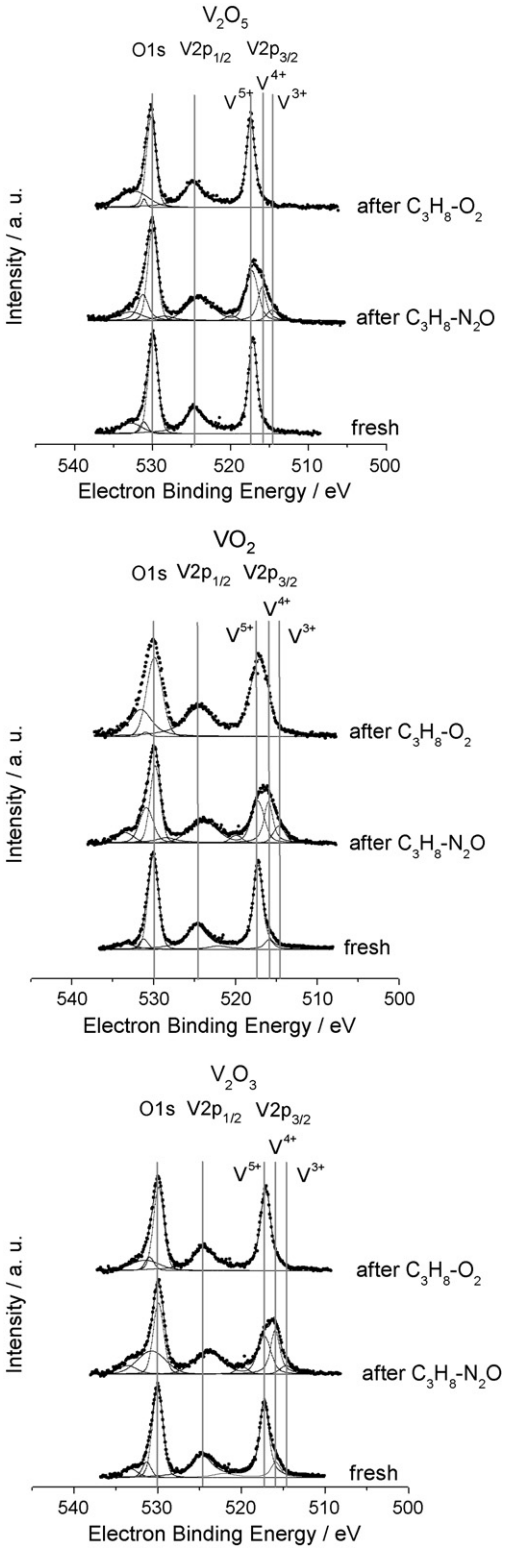

Fig. 6. XPS spectra in the O 1s and V 2p region of V_2O_5, VO_2 and V_2O_3: fresh as well as after the ODP reaction with O_2 or N_2O at 773 K. $C_3H_8/O_2/Ne$ = 40/20/40 or $C_3H_8/N_2O/Ne$ = 40/40/20, $X(C_3H_8) < 5\%$, $X(O_2) < 10\%$, $X(N_2O) < 10\%$.

vanadium oxides and samples used for the ODP reaction at 773 K with O_2 and N_2O. For all the fresh vanadium oxides, V^{5+} is the main vanadium state. The presence of V^{5+} in the fresh VO_2 and V_2O_3 may be related to the oxidation of near surface layers with

Table 3
Near surface composition derived from ex situ XPS analysis of different vanadium oxides in fresh state as well as after ODP with O_2 and N_2O at $T = 773$ K ($X(C_3H_8) < 5\%$, $X(O_2) < 10\%$, $X(N_2O) < 10\%$)

Catalysts	Near surface vanadium concentration from ex situ XPS			
	Fresh	After ODP with O_2		After ODP with N_2O
		$C_3H_8/O_2/Ne = 40/20/40$	$C_3H_8/O_2/Ne = 40/10/50$	$C_3H_8/N_2O/Ne = 40/40/20$
V_2O_5	V^{5+} (100%)	V^{5+} (100%)	V^{5+} (66 %), V^{4+} (26 %), V^{3+} (8%)	V^{5+} (58%), V^{4+} (32%), V^{3+} (10%)
VO_2	V^{5+} (90%), V^{4+} (10%)	V^{5+} (100%)		V^{5+} (47%), V^{4+} (37%), V^{3+} (16%)
V_2O_3	V^{5+} (83%), V^{4+} (17%)	V^{5+} (100%)		V^{5+} (47%), V^{4+} (44%), V^{3+} (9%)

air. Small amounts of V^{4+} were observed in fresh VO_2 and V_2O_3. V^{3+} was not identified in the fresh samples, even in V_2O_3.

However, at least 8% near surface vanadium cations are stabilized in trivalent oxidation state (V^{3+}), when vanadium oxides were used for the ODP reaction at 773 K using N_2O as oxidant. Additionally, ca. 30–40% of total near surface vanadium species have a valence state of +4. When O_2 was used for the ODP reaction, no vanadium in trivalent or tetravalent oxidation states was observed. This statement is independent of the initial oxidation state of the samples, i.e. for V_2O_5, VO_2, and V_2O_3.

Based on the XPS results in Table 3, average oxidation states of near surface vanadium under the ODP conditions with O_2 and N_2O were estimated and compared in Fig. 7 to respective values obtained by XRD. This figure clearly illustrates that the average oxidation states of near surface vanadium species under the ODP conditions with O_2 and N_2O are ca. 5 and 4.4, respectively. The respective values for bulk vanadium species are 5 and 3.9 (Fig. 7). The slightly higher average oxidation state of near surface vanadium species as compared to bulk vanadium species (4.4 versus 3.9) after the ODP with N_2O may be due to the fact that for ex situ XPS tests, the samples contacted to air at room temperature and, therefore, are slightly oxidized. Summarizing, it is obvious that both near surface and bulk vanadium species are more oxidized in the presence of O_2 than with N_2O.

3.3. Influence of oxidizing agent on catalytic performance and catalyst composition

The section evaluates the role of reaction-induced changes of vanadium oxides and the nature of oxygen species (lattice oxygen and adsorbed oxygen) in tuning propene selectivity in the ODP reaction. In the beginning, the results of steady-state ODP studies over individual vanadium oxides with O_2 and N_2O as well as of detailed catalyst characterization by ex situ XPS, in situ UV–vis, and in situ XRD are discussed together, in order to elaborate the influence of reaction conditions on catalyst composition (surface and bulk) and respective changes in catalytic performance. Hereafter, the results of isotopically labeled experiments are presented and discussed with the aim to identify selective and non-selective reaction pathways.

3.3.1. Reduction degree and catalytic performance

The XRD and XPS results in Fig. 3, and Fig. 6 as well as in Table 1, and Table 3 evidence that irrespective of the initial state of the vanadium oxides (V_2O_3, VO_2 or V_2O_5), the oxidation state of vanadium (near surface and bulk) is close to +5 after ODP using O_2. The observed structural changes of the individual vanadium oxides under the ODP conditions are

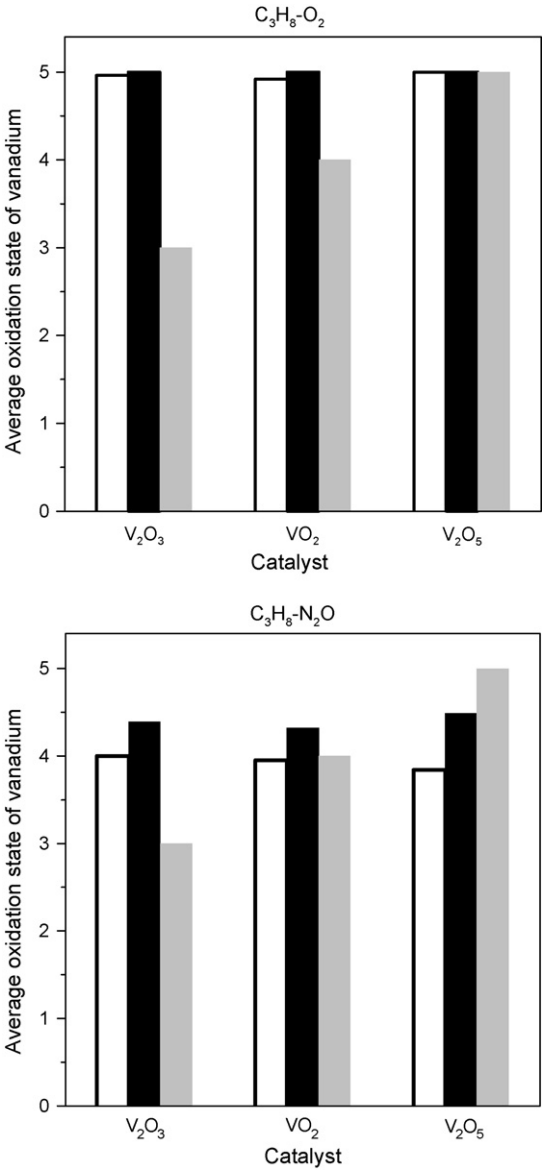

Fig. 7. Estimated average oxidation states of vanadium from in situ XRD (open bars) and ex situ XPS (black bars) after performing ODP tests at 773 K: $C_3H_8/O_2/Ne = 40/20/40$, $C_3H_8/N_2O/Ne = 40/40/20$, $X(C_3H_8) < 5\%$, $X(O_2) < 10\%$, $X(N_2O) < 10\%$. The grey bars represent theoretical oxidation states of vanadium in V_2O_3, VO_2 and V_2O_5.

explained as follows. According to the well-accepted Mars-van Krevelen sequence of the ODP reaction over vanadia-based catalysts [5,20–25], C_3H_8 removes lattice oxygen from vanadium oxides yielding C_3H_6, H_2O and a reduced vanadium center (Eq. (1)). Subsequently, the lattice oxygen is replenished by gas-phase oxygen in a re-oxidation step (Eq. (2)). Since the average oxidation state of near surface and bulk vanadium species is close to +5 for all the individual vanadium oxides having been applied for the ODP reaction with O_2 at 773 K (Fig. 7), it is concluded that the reaction pathway in Eq. (2) is faster than in Eq. (1), i.e. oxidation of reduced vanadium by O_2 is faster than reduction of oxidized vanadium by C_3H_8:

$$C_3H_8 + [O] \xrightarrow{k_{C_3H_8}} C_3H_6 + H_2O + [\,] \quad (1)$$

$$O_2 + 2[\,] \xrightarrow{k_{O_2}} 2[O] \quad (2)$$

$$N_2O + [\,] \xrightarrow{k_{N_2O}} [O] + N_2 \quad (3)$$

where [O] stands for lattice oxygen of vanadium oxide and [ ] corresponds to an anion vacancy after removing of lattice oxygen from the oxide.

Upon replacing of O_2 by N_2O, the average oxidation state of bulk and near surface vanadium after the ODP reaction decreases to between +3.9 and +4.4 (Fig. 7). At this stage it is important to stress that the amount of oxygen atoms in the C_3H_8–O_2 and C_3H_8–N_2O feed mixtures was the same (see Section 2.2). Taking into account this experimental condition, the lower oxidation state of bulk and near surface vanadium in the presence of N_2O as compared to O_2 is related to the lower oxidizing ability of N_2O for reoxidation of reduced vanadium oxides (Eq. (3)). This conclusion is in agreement with our previous results for VO_x/MCM-41 [6] and VO_x/γ-Al_2O_3 [5] catalytic materials, where lower rates of propane consumption were found with N_2O than with O_2.

The results of steady-state ODP studies in Fig. 2 suggest a complex reaction scheme of parallel and consecutive steps for the ODP reaction using either O_2 or N_2O. The scheme is presented in Fig. 8. According to this scheme, the importance of direct (not via consecutive propene oxidation) propane oxidation to CO_x (mainly to CO_2) is significantly higher in the presence of O_2 than in N_2O. Hence, the catalytic performance is determined by the oxidant activation, since this is a necessary stage for the heterogeneous reactions of partial oxidation [8,26]. In order to derive further insights into the role of O_2 in CO_x formation, catalytic tests were performed using a $C_3H_8/O_2/Ne = 40/10/50$ reaction feed, i.e. oxygen concentration was reduced as compared to the standard reaction feed ($C_3H_8/O_2/Ne = 40/20/40$). These experiments are also crucial for elucidating the effect of the degree of reduction of vanadium species on the ODP performance. As shown in Table 3 the relative concentration of V^{5+} decreases from 100 to 66%, while that of V^{4+} and V^{3+} increases from 0 to 26% and from 0 to 8%, respectively, when the ODP reaction is performed with a partial oxygen pressure of 10 kPa instead of 20 kPa. Similar relative concentrations of near surface vanadium were found after performing the ODP reaction over V_2O_5 with N_2O (Table 3). Hence, the reduction degree of near surface vanadium in V_2O_5 was similar in $C_3H_8/N_2O/Ne = 40/40/20$ and $C_3H_8/O_2/Ne = 40/10/50$ reaction feeds.

The selectivity–conversion plots over V_2O_5 and V_2O_3 with the two feeds containing 10 and 20 vol.% of oxygen are shown in Fig. 9. The respective data for an N_2O-containg feed are also

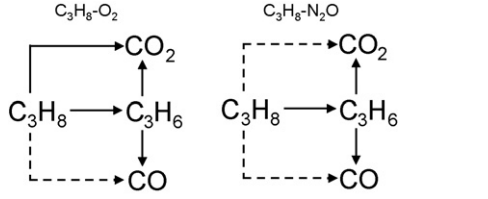

Fig. 8. Suggested reaction scheme of propane oxidation with O_2 and N_2O. Solid lines represent major reaction pathways, while dotted lines indicate minor reaction pathways.

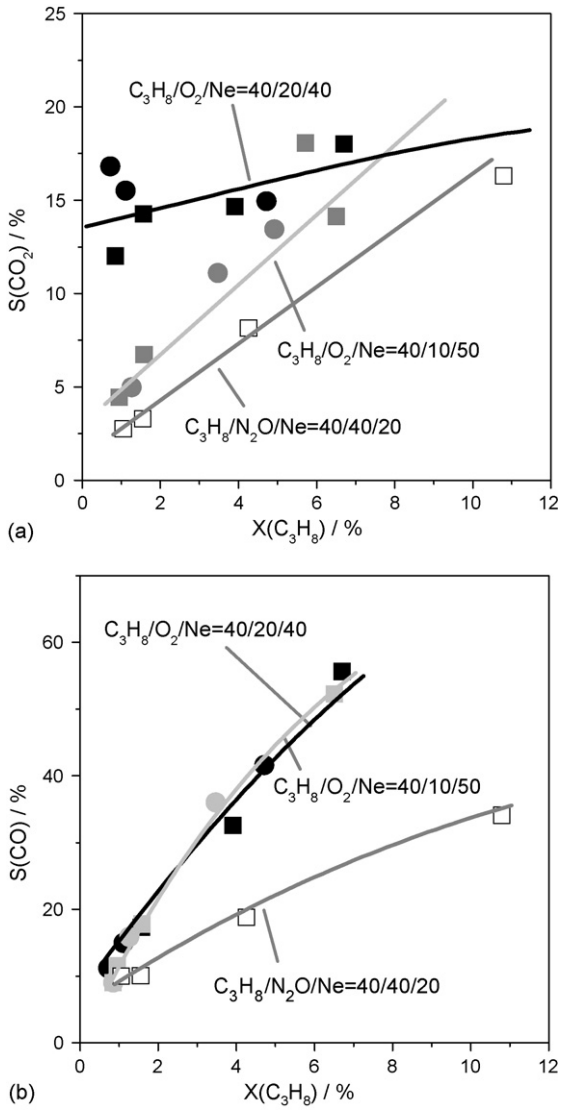

Fig. 9. Selectivity towards CO_2 (a) and CO (b) measured at different degrees of propane conversion over V_2O_5 (■, ■),and V_2O_3 (●, ●) (T = 773 K, $C_3H_8/O_2/Ne = 40/20/40$ or $C_3H_8/O_2/Ne = 40/10/50$). Black and grey symbols for the feeds containing 20% and 10% oxygen, respectively.

presented for comparison. It is clearly seen that the CO selectivity is not significantly influenced by oxygen partial pressures (Fig. 9(b)). However, there is a significant difference in CO_2 selectivity between the O_2- and N_2O-containing feeds. In contrast to the CO selectivity, the CO_2 selectivity at a zero degree of propane conversion decreases strongly when the oxygen partial pressure is reduced (Fig. 9(a)). This result indicates that the relevance of a direct route (not via consecutive propene oxidation) of propane oxidation to CO_2 is a function of the oxygen partial pressure: the higher the pressure, the higher the contribution of the direct propane oxidation to total CO_2 production, and the lower the consecutive propene oxidation to CO_2. In agreement with this statement, the CO_2 selectivity increases with an increased propane conversion stronger for reaction with the $C_3H_8/O_2/Ne = 40/10/50$ reaction feed (Fig. 9(a)) as compared to the $C_3H_8/O_2/Ne = 40/20/40$ reaction feed. Again as for the CO selectivity, the CO_2 selectivity is lower with N_2O than with O_2. The above results clearly show that oxygen partial pressure plays an important role for deriving low CO_x selectivity. However, the nature of oxidizing agent (O_2 versus N_2O) has a stronger influence on CO_x selectivity than the variation of the partial pressure of O_2.

In order to quantify the effect of oxidizing agent (N_2O and O_2) and the oxygen partial pressure on the initial (at zero degree of propane conversion) propene selectivity and on the catalyst ability for consecutive propene oxidation, the respective selectivity–conversion plots (e.g. Fig. 2(a)) were treated according to the following procedure. In the range of propane conversion from 0 to 7%, propene selectivity was approximated by a linear function of propane conversion (Eq. (4)):

$$S(C_3H_6) = S(C_3H_6)_{initial} - A \times X(C_3H_8) \quad (4)$$

where $S(C_3H_6)_{initial}$ is the initial propene selectivity and A corresponds to the catalyst ability for consecutive propene oxidation.

The results in Table 4 indicate that a higher initial propene selectivity is achieved with N_2O than with O_2 for all the studied vanadium oxides using $C_3H_8/N_2O/Ne = 40/40/20$ and $C_3H_8/O_2/Ne = 40/20/40$ reaction feeds. When the oxygen partial pressure decreases from 20 to 10 kPa, the initial propene selectivity increases and is close to that with 40 kPa of N_2O. However, the catalyst ability for consecutive propene oxidation is not influenced by the oxygen partial pressures. Consecutive propene oxidation is significantly lower when O_2 is replaced by N_2O. Thus, the following important effects of oxidizing agent on the ODP reaction were established:

(i) direct C_3H_8 combustion to CO_2 is strongly inhibited in the presence of N_2O and by reducing oxygen partial pressure;
(ii) initial C_3H_6 selectivity is improved by using N_2O instead of O_2, or by reducing O_2 partial pressure;
(iii) the decrease in C_3H_6 selectivity with increasing degree of C_3H_8 conversion is less marked with N_2O than with O_2-containing feeds.

Based on the above discussion, the degree of reduction of vanadium species (bulk and surface) is suggested to be a key factor influencing initial propene selectivity. However, the reduction degree is not the only catalyst property, which determines the catalyst ability for consecutive propene oxidation to CO_x. This conclusion is based on the fact that the reduction degree of vanadium species in V_2O_5 after the ODP reaction using $C_3H_8/N_2O/Ne = 40/40/20$ and $C_3H_8/O_2/Ne = 40/10/50$ feeds is similar (Table 3) but the catalytic performance is different (Fig. 9, Table 4). The difference between O_2- and N_2O-containing ODP feeds in the catalytic performance of vanadium oxides (Fig. 2, Table 4) may be partially related to the nature of active oxygen species originating from O_2. To support this assumption, we performed transient experiments with isotopically labeled $^{18}O_2$ using a SSITKA (steady-state isotopic transient kinetic analysis) technique. The idea is to follow distribution of non-labeled (^{16}O) oxygen (lattice oxygen of vanadium oxides) and labeled (^{18}O) oxygen (adsorbed oxygen) in carbon dioxide. The results are presented and discussed below.

3.3.2. Oxygen species in the ODP reaction

The transients of oxygen isotopic traces upon switching from $^{16}O_2/Ar/Ne = 2/96/2$ to $^{18}O_2/Ar/Ne = 2/96/2$ over V_2O_5 are shown in Fig. 10(a). The concentration of non-labeled oxygen ($^{16}O_2$) decreases, while the concentration of labeled oxygen ($^{18}O_2$) increases. No $^{18}O^{16}O$ was detected over V_2O_5. The absence of $^{18}O^{16}O$ and the presence of $^{16}O_2$ in the $^{18}O_2$-containing feed indicate irreversible dissociative oxygen adsorption [21]. However, traces of $^{18}O^{16}O$ were observed, when oxygen isotopic exchange was studied in the presence of C_3H_8. In this experiment, isotopic transients were monitored upon switching from a $C_3H_8/^{16}O_2/Ar/Ne = 4/2/92/2$ mixture to a $C_3H_8/^{18}O_2/Ar/Ne = 4/2/92/2$. The respective results are presented in Fig. 10(b). The presence of $^{18}O^{16}O$ implies that oxygen interaction with V_2O_5 in the presence of C_3H_8 occurs dissociatively and reversible. The difference in oxygen distribution in the absence and presence of C_3H_8 may be

Table 4
Initial C_3H_6 selectivity ($S(C_3H_6)_{initial}$) and catalytic ability (A) for consecutive C_3H_6 oxidation ($T = 773$ K, $C_3H_8/O_2/Ne = 40/20/40$, $C_3H_8/O_2/Ne = 40/10/50$, $C_3H_8/N_2O/Ne = 40/40/20$) according to Eq. (4)

Catalysts	Initial C_3H_6 selectivity (%) ($S(C_3H_6)_{initial}$)			Ability for consecutive C_3H_6 oxidation[a] (A)		
	20% O_2	10% O_2	40% N_2O	20% O_2	10% O_2	40% N_2O
V_2O_5	81	88	89	8.2	8.5	3.4
VO_2	81		88	7.1		3.3
V_2O_3	75	89	92	7.1	10	3.5

[a] $\Delta S(C_3H_6)/\Delta X(C_3H_8)$ calculated in the range of propane conversions from 0 to 7%.

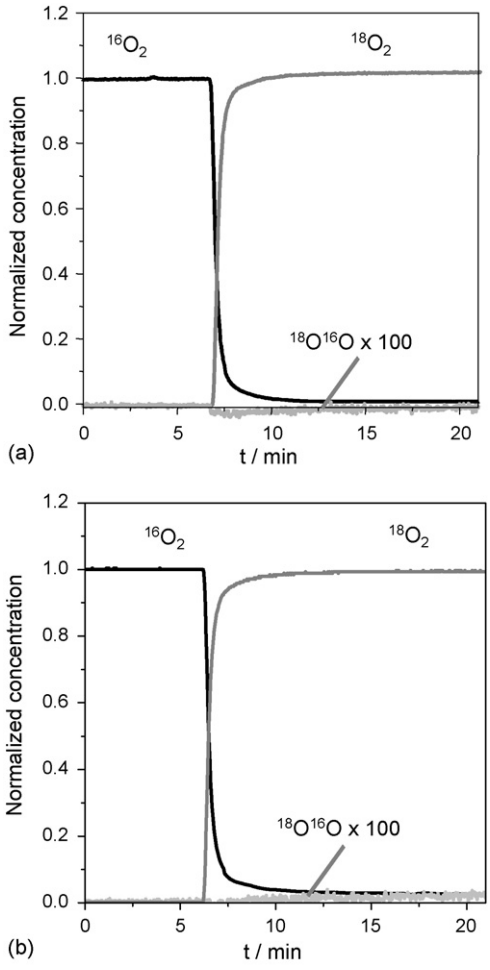

Fig. 10. Oxygen transients over V_2O_5 at 773 K upon switching: from $^{16}O_2$/Ar/Ne = 2/94/2 to $^{18}O_2$/Ar/Ne = 2/94/2 (a) or from C_3H_8/$^{16}O_2$/Ar/Ne = 4/2/92/2 to C_3H_8/$^{18}O_2$/Ar/Ne = 4/2/92/2 (b).

related to the fact that anion vacancies are created in the presence of C_3H_8. These reduced vanadium are active for O_2 adsorption, which may occur differently as compared to the interaction with oxidized V_2O_5.

For analyzing the possible role of lattice and adsorbed oxygen species in CO_2 formation, two different isotopic experiments were performed over V_2O_3: a) $V_2{}^{16}O_3$ was heated in a Ne flow up to 773 K followed by feeding a C_3H_8/$^{18}O_2$/Ar/Ne = 4/2/92/2 mixture for 15 min (Fig. 11(a)) and b) hereafter a C_3H_8/$^{16}O_2$/Ar/Ne = 4/2/92/2 mixture was fed over the catalyst at the same temperature for ca. 2 h followed by switching to the reaction feed with isotopically labeled oxygen (C_3H_8/$^{18}O_2$/Ar/Ne = 4/2/92/2) (Fig. 11(b)). Experiment b was also performed over V_2O_5 (Fig. 11(c)).

The discussion of transient responses in Fig. 11 starts with the description of the results of C_3H_8–$^{18}O_2$ interactions with fresh V_2O_3 containing ^{16}O (experiment (a), Fig. 11(a)). Three differently labeled carbon dioxides were observed: $C^{16}O_2$, $C^{16}O^{18}O$, and $C^{18}O_2$. It has to be highlighted that in all the experiments, concentrations of isotopically labeled carbon dioxides were normalized with respect to steady-state concentration of $C^{16}O_2$ after 2 h on stream in a C_3H_8/$^{16}O_2$/

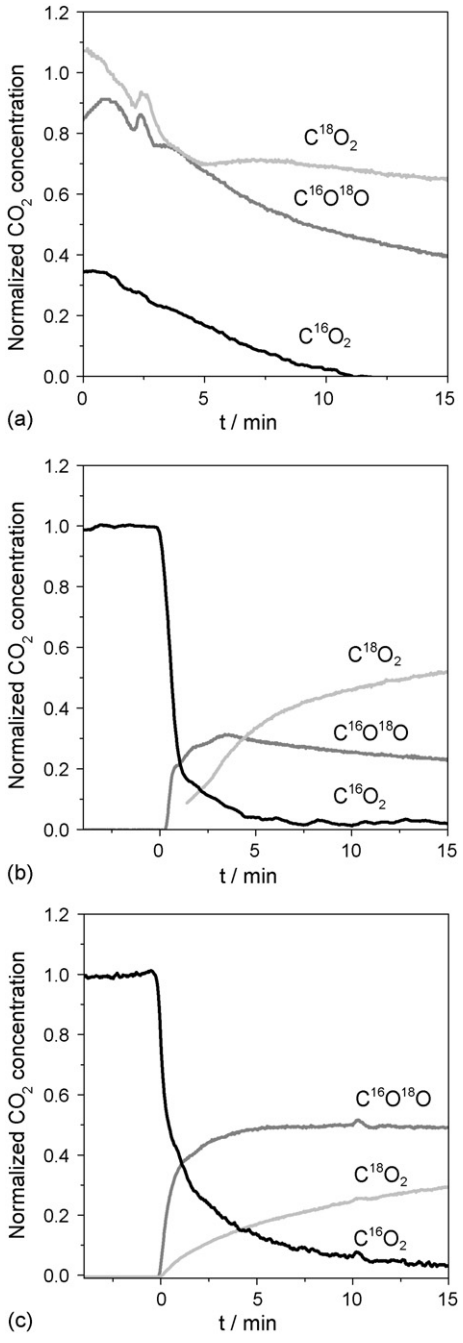

Fig. 11. Carbon dioxide transients over fresh V_2O_3 (20 mg) (a), V_2O_3 after 2 h in C_3H_8–$^{16}O_2$ (b) and V_2O_5 (50 mg) after 2 h in C_3H_8–$^{16}O_2$ (c) at 773 K upon switching from C_3H_8/$^{16}O_2$/Ar/Ne = 4/2/92/2 to C_3H_8/$^{18}O_2$/Ar/Ne = 4/2/92/2.

Ar/Ne = 4/2/92/2 flow. Since catalyst deactivation was observed during 2 h on stream, the total concentration of $C^{18}O_2$, $C^{18}O^{16}O$ and $C^{16}O_2$ during first 15 min on stream in Fig. 11(a) is higher than one. $C^{16}O_2$ has the lowest concentration among all isotopically labeled carbon dioxides. The concentrations of $C^{16}O^{18}O$, and $C^{18}O_2$ are similar. Moreover, the transient response of $C^{16}O_2$ decreases and approaches zero after 10 min on stream in the C_3H_8/$^{18}O_2$/Ar/Ne = 4/2/92/2 mixture (Fig. 11(a)). The transients of $C^{18}O^{16}O$ and $^{18}CO_2$ fall slightly with time on stream, too. However, their concentrations are still high after 15 min on stream in the

$C_3H_8/^{18}O_2/Ar/Ne = 4/2/92/2$ flow. This result indicates that there are different reaction pathways leading to carbon dioxide.

In isotope experiments over V_2O_3 and V_2O_5 after 2 h on stream in a $C_3H_8/^{16}O_2/Ar/Ne = 4/2/92/2$ mixture (Fig. 11(b) and (c)), $C^{18}O^{16}O$ and $^{18}CO_2$ start to be formed immediately after switching from $C_3H_8/^{16}O_2/Ar/Ne = 4/2/92/2$ to $C_3H_8/^{18}O_2/Ar/Ne = 4/2/92/2$ mixture. The presence of ^{16}O in $C^{16}O_2$, and $C^{16}O^{18}O$ upon feeding $C_3H_8/^{18}O_2/Ar/Ne$ flow indicates the participation of lattice oxygen of vanadium oxides in carbon dioxide formation. The transient response of $C^{18}O^{16}O$ increases strongly with time approaching a maximum after ca. 5 min on stream followed by a slow decay, while the transient response of $C^{18}O_2$ increases considerably slower but continuously. The permanent increase of $C^{18}O_2$ production and the decrease in $C^{16}O_2$ formation are attributed to replacing of non-labeled (^{16}O) lattice oxygen in VO_x species by labeled (^{18}O) ones. However, the lattice oxygen is not the only species participating in carbon dioxide formation. It is suggested that adsorbed oxygen species contribute to carbon dioxide formation, too. This assumption is based on the following discussion.

Fig. 11(a) shows that the concentration of $C^{18}O_2$ and $C^{16}O^{18}O$ is always higher than that of $C^{16}O_2$ even immediately ($t \sim 0$) upon feeding the $C_3H_8/^{18}O_2/Ar/Ne = 4/2/92/2$ flow over V_2O_3 containing non-labeled (^{16}O) oxygen. This means that either oxygen species formed from gas-phase $^{18}O_2$ are more active for carbon dioxide formation than lattice oxygen (^{16}O) of V_2O_3 or their concentration is higher. Another important observation is the difference in the temporal profiles of $C^{16}O_2$ and $C^{16}O^{18}O$ in Fig. 11 for all experiments. These two isotopically labeled carbon dioxides contain ^{16}O, which originates from the lattice of vanadium oxides. While the concentration of $C^{16}O_2$ drops to zero within first 10–15 min on stream in the $C_3H_8/^{18}O_2/Ar/Ne = 4/2/92/2$ flow, the concentrations of both $C^{16}O^{18}O$ and $C^{18}O_2$ are much higher and similar to each other. Therefore, similar surface concentration of lattice ^{16}O and ^{18}O oxygen should be expected after 15 min on stream in the $C_3H_8/^{18}O_2/Ar/Ne = 4/2/92/2$ flow, if lattice oxygen would be the only species participating in carbon dioxide formation. In this case, $C^{16}O_2$ should be also observed over the same period of time as $C^{16}O^{18}O$, which is in contradiction to the results in Fig. 11. Thus, it is suggested that in addition to lattice oxygen adsorbed oxygen species should participate in carbon dioxide formation. This statement is supported by the catalytic results in Figs. 2 and 9. These figures clearly demonstrate that CO_2 formation is considerably decreased upon replacing O_2 by N_2O or by decreasing O_2 partial pressure. It is suggested that the decreased CO_2 production upon reducing oxygen partial pressure in Fig. 9 is due to a decrease in concentration of adsorbed (non-selective) oxygen species. The effect of N_2O on reduced CO_2 production in Fig. 2 can be understood taking the below discussion into account.

According to Bielanski and Haber [8] O_2 activation over reducible metal oxides occurs via a complex sequence of redox processes until O^{2-} (lattice oxygen) is formed. This species actively participates in the ODP reaction over vanadium-based catalysts [5,8,20,22,27,28]. However, O^{2-} is not the only species formed from O_2. Adsorbed oxygen species were suggested as non-selective species for the ODP reaction over V–Mg–O [29,30] and $Mn_{0.18}V_{0.3}Cr_{0.23}W_{0.26}O_x$–$Al_2O_3$ [25] catalytic materials. Density function theory calculations predict that gas-phase oxygen adsorbs molecularly over anion vacancy of reduced V_2O_5 [31,32]. This molecular adsorbed oxygen dissociates further yielding lattice oxygen species. In contrast to O_2 adsorption, N_2O decomposition over reducible metal oxides yields mononuclear oxygen species: O^- or O^{2-}. Hence, the stronger tendency towards CO_x formation in the presence of O_2, as compared to N_2O, is possibly related to the formation of adsorbed molecular oxygen on reduced VO_x surface from gas-phase oxygen. However, in order to draw a definitive conclusion on the nature of selective and non-selective oxygen species in the ODP reaction, a deeper mechanistic analysis is required and is presently worked on.

4. Conclusions

Our mechanistic investigation of the ODP reaction with O_2, $^{18}O_2$ and N_2O over V_2O_3, VO_2 and V_2O_5 by means of steady-state catalytic tests as well as in situ UV–vis, in situ XRD and ex situ XPS analysis elucidated the importance of reaction-induced changes of the vanadium oxides for their catalytic performance. The obtained conclusions provided deeper insights into the vanadium oxides catalyzed ODP reaction. The main conclusions are:

- In order to adequately establish structure–reactivity relationships in the ODP reaction over easily reducible/reoxidisable oxides, catalyst characterization should be performed at controlled degrees of propane and oxidant conversion; concentration gradients of feed components along the catalyst bed are to be minimized.
- Steady-state ODP product selectivities over individual vanadium oxides at 773 K are not determined by the nature of fresh vanadium oxide. This is governed by reaction-induced changes of the bulk and surface states of the oxides under the ODP conditions.
- Bulk and near surface composition of V_2O_3, VO_2 and V_2O_5 under the ODP conditions is controlled by the applied oxidizing agent (O_2 or N_2O). For an oxygen ($C_3H_8/O_2 = 2$) containing mixture, vanadium species are stabilized in penta- and tetravalent oxidation states, with the former being the main one. The oxidation state of vanadium reduces in the presence of N_2O.
- The oxidizing agent tunes the catalytic performance of the studied vanadium oxides. As compared to O_2-containing feeds, direct C_3H_8 oxidation to CO and CO_2 (mainly) as well as consecutive C_3H_6 oxidation to CO_x are drastically reduced in the presence of N_2O. The corresponding improved initial C_3H_6 selectivity can be related to the degree of reduction of vanadium sites; the higher the degree, the higher the selectivity. It is assumed that also the nature of oxygen species originated from O_2 and N_2O differs and plays a role in consecutive C_3H_6 and direct C_3H_8 oxidation.

Acknowledgements

Support by Deutsche Forschungsgemeinschaft (DFG) within the collaborative research center ''Structure, dynamics and reactivity of transition metal oxide aggregates'' (Sonderforschungsbereich 546) is greatly appreciated. The authors also thank to Miss Olga Schulz for technical assistance in the catalytic experiments.

References

[1] M.A. Bañares, Catal. Today 51 (1999) 319.
[2] M. Baerns, O.V. Buyevskaya, Erdöl Erdgas Kohle 116 (2000) 25.
[3] O.V. Buyevskaya, M. Baerns, Catalysis 16 (2002) 155.
[4] M. Baerns, G. Grubert, E.V. Kondratenko, D. Linke, U. Rodemerk, Oil Gas-Eur. Magn. 1 (2003) 36.
[5] E.V. Kondratenko, M. Baerns, Appl. Catal. A 222 (2001) 133.
[6] E.V. Kondratenko, M. Cherian, M. Baerns, X. Su, R. Schlögl, X. Wang, I.E. Wachs, J. Catal. 234 (2005) 131.
[7] K. Tarama, S. Teranishi, S. Yoshida, N. Tamura, in: Proceedings of the 3rd International Congress on Catalysis, vol. 1, 1964, p. 282.
[8] A. Bielanski, J. Haber, Oxygen in Catalysis, Marcel Dekker, New York, 1991, p. 320.
[9] U.S. Ozkan, T.A. Harris, B.T. Schilf, Catal. Today 33 (1997) 57.
[10] D.S. Su, R. Schlögl, Catal. Lett. 83 (2002) 115.
[11] B.P. Barbero, L.E. Cadus, L.U. Hilaire, Appl. Catal. A 246 (2003) 237.
[12] M. Occhiuzzi, D. Cordischi, R. Dragone, J. Solid State Chem. 178 (2005) 1551.
[13] M. Gasior, B. Grzybowska-Swierkosz, Vanadia Catalysts for Processes of Oxidation of Aromatic Hydrocarbons, Polish Scientific Publishers, Warsaw, 1984, p. 133.
[14] M. Havecker, N. Pinna, K. Weiss, H. Sack-Kongehl, R.E. Jentoft, D. Wang, M. Swoboda, U. Wild, M. Niederberger, J. Urban, D.S. Su, R. Schlögl, J. Catal. 236 (2005) 221.
[15] J. Mendialdua, R. Casanova, Y. Barbaux, J. Electron. Spectrosc. Relat. Phenom. 71 (1995) 249.
[16] G.A. Sawatzky, D. Post, Phys. Rev. B 20 (1979) 1546.
[17] M. Demeter, M. Neumann, W. Reichelt, Surf. Sci. 454–456 (2000) 41.
[18] G. Silversmit, D. Depla, H. Poelman, G.B. Marin, R. De Gryse, J. Electron. Spectrom. Relat. Phenom. 135 (2004) 167.
[19] A.-C. Dupuis, M. Abu Haija, B. Richter, H. Kuhlenbeck, H.-J. Freund, Surf. Sci. 539 (2003) 99–112.
[20] S.L.T. Andersen, Appl. Catal. A 112 (1994) 209.
[21] K. Chen, A. Khodakov, J. Yang, A.T. Bell, E. Iglesia, J. Catal. 186 (1999) 325–333.
[22] K. Chen, A.T. Bell, E. Iglesia, J. Phys. Chem. B 104 (2000) 1292.
[23] M.D. Argyle, K. Chen, A.T. Bell, E. Iglesia, J. Catal. 208 (2002) 139.
[24] R. Grabowski, J. Sloczyñski, N.M. Grzesik, Appl. Catal. A 232 (2002) 277.
[25] E.V. Kondratenko, M. Cherian, M. Baerns, Catal. Today 99 (2005) 59.
[26] G.I. Panov, A.K. Uriarte, M.K. Rodkin, V.I. Sobolev, Catal. Today 41 (1998) 365.
[27] A. Pantazidis, S.A. Bucholz, H.W. Zanthoff, Y. Schuurman, C. Mirodatos, Catal. Today 40 (1998) 207.
[28] E.V. Kondratenko, O.V. Buyevskaya, M. Baerns, Topics Catal. 15 (2001) 175.
[29] H.W. Zanthoff, S.A. Buchholz, A. Pantazidis, C. Mirodatos, Chem. Eng. Sci. 54 (1999) 4397.
[30] D. Creaser, B. Andersson, R.R. Hudgins, P.L. Silveston, J. Catal. 182 (1999) 264.
[31] K. Hermann, M. Witko, in: D.P. Woodruff (Ed.), The Chemical Physics of Solid Surfaces, Elsevier Science, Amsterdam, 2001, p. 136.
[32] R. Tokarz-Sobieraj, M. Witko, R. Grybos, Catal. Today 99 (2005) 241.